



Oxidation is Key for Black Carbon Surface Functionality and Nutrient Retention in Amazon Anthrosols

**Biqing Liang^{1,2*}, Chung-Ho Wang¹, Dawit Solomon², James Kinyangi^{2,3},
Flavio J. Luizão⁴, Sue Wirick⁵, Jan O. Skjemstad⁶
and Johannes Lehmann^{2*}**

¹*Institute of Earth Sciences, Academia Sinica, Nangang, Taipei 11129, Taiwan ROC.*

²*Department of Crop and Soil Sciences, Cornell University, Ithaca, NY 14853, USA.*

³*International Livestock Research Institute (ILRI), P.O. Box 30709, 00100, Nairobi, Kenya.*

⁴*Instituto Nacional de Pesquisa da Amazônia (INPA), 69011-970 Manaus, Brazil.*

⁵*Department of Physics and Astronomy, State University of New York at Stony Brook, NY, USA.*

⁶*CSIRO Land and Water, PMB No. 2, Glen Osmond SA 5064, Australia.*

Authors' contributions

This work was carried out in collaboration between all authors. Authors BL and JL designed the study and wrote the article. Authors BL, DS, JK, SW and JL performed the NEXAFS, authors BL, CHW and JL analyzed the data. FJL provided the sample. Author JOS performed the NMR. All authors read and approved the final manuscript.

Research Article

Received 30th September 2012

Accepted 16th October 2012

Published 10th April 2013

ABSTRACT

Aims: Soil black carbon (BC) has been shown to possess large amounts of cation exchange sites and surface charge, and is viewed as a potential soil amendment to improve nutrient retention and for pollutant remediation. This study investigated the nano-scale distribution of reactive functional groups and the binding of cations on the surface of micron-size BC particles, identified the key processes, and explored the sources of surface functionality and their relative contribution to cation exchange capacity (CEC).

Materials and Methods: Elemental microprobe and synchrotron-based Scanning Transmission X-ray Spectromicroscopy (STXM) coupled with Near Edge X-ray Absorption Fine Structure (NEXAFS) spectroscopy were used for nano-scale mapping of

*Corresponding author: Email: Bqliang@earth.sinica.edu.tw; CL273@cornell.edu;

cations and reactive functional groups, and further distinction of the sources of reactive functional groups generated either by oxidation of BC surfaces or by adsorption of non-BC organic matter onto the BC surfaces. Their respective contribution to cation adsorption was obtained using a depth profile of a BC-rich Anthrosol from the central Amazon, Brazil.

Results and Discussion: Adsorption of Non-BC organic matter is more dominant on the surface of BC particle in topsoil as evidenced by a stronger signal of microbial biomass and humic substances extracts. In comparison, a greater level of oxidation was found on the outerlayer of BC particles in subsoil horizons. Organic C in subsoils was found to generate 23-42% more CEC per unit C than topsoil. Based on CEC per unit C, the capacity of BC in creating CEC was 6-7 times higher than Non-BC, and the BC in deeper horizons had up to 20% higher CEC than the topsoil horizon. Near BC surfaces, higher ratios of Ca/C and K/C in subsoil than topsoil horizons reinforce the observation that BC in subsoil horizons had a higher capacity in binding cations and creating CEC than in the topsoil horizon.

Conclusions: Oxidation of BC is suggested to be more efficient and important for creating CEC than the adsorption of non-BC onto BC surfaces, thus identified as being key for BC surface functionality and nutrient retention in Amazon Anthrosols.

Keywords: Adsorption; black carbon; nutrient retention; oxidation; surface functionality; synchrotron-based scanning transmission X-ray spectromicroscopy (STXM); near edge X-ray absorption fine structure (NEXAFS) spectroscopy.

1. INTRODUCTION

Black carbon (BC), thermally altered residue from incomplete combustion of organic matter, exists ubiquitously in the environment in various forms from partially charred carbonaceous materials to highly condensed soot and graphite [1]. Black C in soils is of great biogeochemical significance [2], not only important to global C cycling and sequestration [3-5], but also to environmental pollutant filtration especially in hydrological systems [6, 7] and to soil fertility improvement [8,9]. The adsorption of organic pollutants [10-14], dissolved organic matter [15] and base cations [16] by BC surfaces and their high surface area of up to $10^5 \text{ m}^2 \text{ g}^{-1}$ [17] may explain why BC in Brazilian Amazonian anthropogenic soils (Anthrosols) plays a key role for their sustainable fertility in high leaching environment [8]. Higher nutrient retention and nutrient availability has been found after additions of biomass-derived BC to soil, likely resulting from higher cation exchange capacity (CEC), substantial increase of surface area and direct additions of nutrient [9,16].

Only recently, direct evidence has been found to explain how BC surface properties contribute to the higher CEC in Anthrosols with high-BC content [16,18]. Significantly higher CEC per unit soil organic C was observed in these Anthrosols compared with adjacent forest soils [19]. While a high surface area for cation adsorption could be one possible explanation, a higher charge density per unit surface area will account for higher abundance of negatively charged functional groups on BC surfaces. High abundance of reactive functional groups in oxidized C form (carboxyl groups etc) was thought to be the main reason for the observed high CEC [16]. The high abundance of reactive functional groups with net negative charge in the pH range of soils may result from two principally different processes: (i) surface oxidation of BC particles themselves; or (ii) adsorption of highly oxidized organic matter onto BC surfaces [18]. It remains unknown to what extent either oxidation or adsorption occurs on BC

surfaces, and therefore, from which source the reactive functional groups and the CEC originate.

Therefore, we investigated the extent to which reactive functional groups originate from either BC oxidation or from adsorption of other Non-BC organic matter in BC-rich Anthrosols. Secondly, we assessed the relative contribution of these two sources to CEC and associated distribution with cations in these soils under a high leaching environment.

2. MATERIALS AND METHODS

2.1 Sites and Soil Sampling

A depth profile was obtained from a BC-rich Anthrosol at the Lago Grande (LG) site near Manaus, Brazil (3° 8' S, 59° 52' W, 40-50 m above sea level), which is an archaeological site dated to 900-1100 years B.P. and covered by an old secondary forest. Soil samples were taken from depths of 0-0.16 m (A, different batch of sample from that in [16]), 0.16-0.43 m (B), 0.43-0.67 m (C), and 0.67-1.20 m (D). Soil samples were subsequently air dried and passed through a 2 mm sieve. One composite sample of BC-poor soil with similar mineralogy was taken from adjacent site top soils as a total of three subsamples. The topsoil horizon (A; Table 1) likely received more recent inputs of external plant residues, compared to the subsoil horizons (B, C and D).

2.2 Cation Exchange Capacity

Both exchangeable cations (EC; base cations Ca, K, Mg, Na) and potential CEC were measured (different batch of measurement from that in [16]) for soil samples from each depth to quantify the available cations and potential sites for cation adsorption. Soil exchangeable cations were determined by replacement of cations with ammonium acetate (1 M, 25 mL for 2.5 g soil), and potential CEC was determined by a leaching and replacement method with ammonium acetate (1 M, total 35 mL for 2.5 g soil) and KCl (2 M, 25 ml for 2.5 g soil) at pH=7 [16]. A ratio of CEC to organic C was used to indicate the capacity of organic matter to create cation adsorption sites. The CEC for BC and Non-BC were derived from their respective proportion (P) and the total CEC (Table 1) and calculated according to the following equation: $P_{BC} * CEC_{BC} + P_{Non-BC} * CEC_{Non-BC} = CEC_C$. Here the P_{BC} is the proportion (P) of BC relative to soil total C, and P_{Non-BC} is the proportion of Non-BC relative to soil total C, both P_{BC} and P_{Non-BC} are known parameters, as the BC contents were assessed by ^{13}C Nuclear Magnetic Resonance (NMR) spectroscopy (as described in later Section 2.3), and the portion of Non-BC was obtained by subtracting the BC content from soil total C content. CEC_C was obtained from dividing soil CEC by soil total C. CEC_{BC} is CEC per unit BC and CEC_{Non-BC} is CEC per unit Non-BC, both remain to be solved. The equations are based on assumption that BC and Non-BC have different capacity contributing to CEC due to their distinct surface chemistry and functionality.

We only have one top soil sample for the adjacent soil, and we use the same CEC_{Non-BC} each time. The key assumption is that the CEC_{Non-BC} is similar for soils with high BC and low BC, and for soil with high BC at different depth. Thus the CEC of Non-BC was tentatively fixed as the same for the BC-rich topsoil (Equation 1) and BC-poor adjacent soil (Equation 2). Based on this assumption, two equations were combined and the variable CEC_{BC} was solved and the tentative constant CEC_{Non-BC} was derived for top soil Depth A. For example, for BC rich Anthrosol top soil (Depth A), we put in the known proportion of BC and Non-BC to the

original equation and have Equation 1: $62.2\% * CEC_{BC} + 37.8\% * CEC_{Non-BC} = 10.1$; as for BC poor adjacent soil, we have Equation 2: $9.3\% * CEC_{BC} + 90.7\% * CEC_{Non-BC} = 3.3$, when we pair up Equation 1 and 2, and we can solve CEC_{BC} equals to 15.0, and CEC_{Non-BC} equals to 2.1. As for BC rich Anthrosol Depth B, we can set up Equation 3 as: $77\% * CEC_{BC} + 23\% * CEC_{Non-BC} = 12.4$. Likewise, we can set up Equation 4 for Depth C as: $76.2\% * CEC_{BC} + 22.8\% * CEC_{Non-BC} = 13.5$ and Equation 5 for Depth D as $77.8\% * CEC_{BC} + 22.2\% * CEC_{Non-BC} = 14.2$. By putting in $CEC_{Non-BC} = 2.1$, we derive CEC_{BC} for depth B, C and D equals to 15.5, 17.1 and 17.8, respectively (Table 1).

To explore the range of CEC_{Non-BC} and validate the estimation accuracy of CEC_{BC} , we also consider CEC_{Non-BC} as an unfixed parameter, and use it new in Equation 2 to pair up equation from each high BC depth. Specifically, the CEC_{Non-BC} could vary for soil with high BC and low BC, and soil with high BC at different depth. The discussion was included in Supplementary information (Table S1). In both fixed and unfixed scenarios for CEC_{Non-BC} , the value of CEC_{BC} varied less than 0.5%, thus the estimation of CEC_{BC} was sound.

2.3 Black Carbon Content

The BC contents were assessed by applying ^{13}C Nuclear Magnetic Resonance (NMR) spectroscopy with cross polarization / magic angle spinning (CP/MAS) after pre-treatment with HF (2%, wt./vol.) for the soil samples from the entire depth profile (horizon A, B, C and D) and the adjacent soil according to Skjemstad et al., [20]. The BC contents were first obtained by running a Molecular Mixing Model developed by Nelson and Baldock [21] and then recalculated with a correction factor of 0.27 for CP observability [22]. The portion of Non-BC was obtained by subtracting the BC content from total soil C content. The relative capacity of BC and Non-BC contributing to total soil CEC was calculated based on their proportion in BC-rich Anthrosol and adjacent soil.

2.4 Specific Surface Area

Specific surface area (SSA) measurements were performed to estimate the surface area available for cation adsorption. The charge density on BC surfaces was calculated by a ratio of CEC to SSA. The SSA was determined by an automated surface area analyzer (ASAP 2020, Micromeritics Instruments Corp., Norcross, GA) by the N_2 multipoint Brunauer-Emmett-Teller (BET) method using the adsorption leg of the isotherm in relative pressure of full range. Five to 20 g of air-dried and dispersed soil were degassed at 90°C until the pressure stabilized at 8 mm Hg, and then equilibrated with N_2 to obtain adsorption and desorption curves [16]. The SSA was expressed as $m^2 g^{-1}$.

2.5 Sample Preparation for Spectroscopic Measurements

Free stable soil aggregates (20 to 200 μm) were misted by humidifier vapor, shock-frozen and subsequently sectioned using a cryo-microtome (Ultracut UTC, Leica Microsystems Inc., Bannockburn, IL) (Lehmann et al., [23] for details). Sections with a thickness of 100 to 200 nm were cut at -55°C using a diamond knife (MS9859 Ultra 458, Diatome Ltd., Biel, Switzerland) at a cutting speed of 0.3 to 1.2 $mm s^{-1}$ (angle of 6°) and transferred to Cu grids (carbon free, 200 mesh, silicon monoxide No. 53002, Ladd Research, Williston, VT) for later spectroscopic analyses.

2.6 Carbon Functional Groups by NEXAFS

Synchrotron-based Scanning Transmission X-ray Spectromicroscopy (STXM) coupled with Near Edge X-ray Absorption Fine Structure (NEXAFS) spectroscopy was used to map the distribution of C functional groups across BC particles within ultra-thin soil aggregate sections at a spatial resolution of 50 nm [18]. Images of C NEXAFS were recorded below and above the carbon K edge (284.3 eV is the binding energy for elemental C) at the X-1A1 end-station of the National Synchrotron Light Source at Brookhaven National Laboratory (Upton, NY). Images taken at different energy levels were stacked and analyzed according to methods described by Lehmann et al., [18] and Liang et al., [16,22]. Cluster analyses were performed to classify sample regions with similar spectral characteristics [24,25].

Each spectrum from the cluster analysis representing different regions was further deconvoluted to quantify the contribution of either BC oxidation or adsorption of Non-BC materials to the total C functional groups, using Extended X-ray Absorption Fine Structure (EXAFS) analysis software Athena 0.8.052 [26]. A demo of deconvoluted spectrum was included in supplementary information (Fig. S1). One arctangent function was fixed at 290 eV with a full width at half maximum (FWHM) of 1.0 eV for modeling the ionization step [27]. Eight diagnostic peaks were fitted with Gaussian functions at 284.3±0.1 (P0, quinone C), 285.1±0.2 (P1, aromatic C), 286.1(P2, unsaturated aromatic C), 286.5±0.2 (P3, phenol C), 287.7±0.2 (P4, ketone carbonyl or aliphatic C), 288.5±0.1 (P5, carboxyl C), 289.3±0.2 (P6, carbonyl C), and 290.6±0.1 (P7, carbonate C) eV for electronic transitions [18,22]. The peak area of each electronic transition was transformed into percentage of each functional group relative to the sum of all functional groups. Peaks 1 and 2 include aromatic and unsaturated aromatic C and were grouped as Aromatic C, which mainly contains stable C=C bonds. Peaks 4, 5, 6 and 7 were combined as the Oxidized C. The relative ratio of Oxidized C to Aromatic C was used to indicate the oxidation level of organic C.

Different spectral features have previously been identified for the studied BC and adsorbed organic materials which showed distinct peak positions [16, 18, 22], and such signal difference was used to distinguish BC oxidation from the adsorption of Non-BC organic matter. Black C regions often contain a dominant peak at 285.0 eV and a well-resolved peak at 286.1 eV, whereas Non-BC materials show a very small peak at 285.0 eV and a distinct shift of the second peak to higher energy (286.7-286.9 eV). Reference spectra for microbial biomass and humic substances extracts were included in two other studies [16, 18]. Deconvolution was done for bacteria and fungi spectra for the first time. Due to the very limited availability of the Synchrotron-based facility and the difficult nature of such type of analysis, only a few samples can be measured by any given research team per year. We presented a set of results for the whole soil depth profile from our multiple investigation efforts, and another set of data is available in the supplemental information (Table S2).

2.7 Elemental Mapping by Microprobe

A microprobe (JEOL-JXA-8900, Pioneer, Japan) with 5 crystal wavelength dispersive spectrometers (WDS, Thermo Electron Corp, Middleton, WI) was used to map the spatial distribution of selected elements (only C, Ca, K are presented here) on soil aggregate cross-sections, using a Vantage analyzer [16]. The measurement voltage was set to 2.0 keV and 10.00 keV for imaging and elemental mapping, respectively, under a magnification of 1500-7000 times. The measurement currents were set at 1.5 and 15 nA. Regions with different abundance of cations were identified and quantified with a color-coded intensity bar.

Electron X-ray dispersive spectrometry (EDS) was also used to perform line-scans across BC regions within aggregate sections for elements including C, Ca, and K. The relative distribution of C and cations (K and Ca) on BC surfaces was expressed as a ratio of cations to C on a count basis.

3. RESULTS AND DISCUSSION

3.1 Soil CEC, Exchangeable Cations and BC Contents

An 11-13% higher CEC was found in the Anthrosol topsoil horizon A ($292 \text{ mmol}_C \text{ kg}^{-1}$) than in subsoil horizons. The amount of exchangeable base cations (EC) in the topsoil horizon A ($127 \text{ mmol}_C \text{ kg}^{-1}$) was 31-57% higher than that in the subsoil, however, from depth B to D, exchangeable base cations showed a 6-20% increase. The C contents decreased by 58% from the topsoil horizon A (29.0 mg g^{-1}) to the subsoil horizon D (18.4 mg g^{-1}). As reflected by the CEC per unit soil C, the organic C in subsoils was 23-42% more effective in creating CEC than the top soil A (Table 1). Coincidentally, EC to C increased 18-37% from depth B to depth D, showing the soil C in the subsoil horizon has higher capacity for nutrient retention.

The proportion of BC per unit total C was 23-25% higher in subsoil horizons (B, C and D) than in the topsoil horizon A, and the proportion of Non-BC was 59-70% higher in the topsoil horizon A than in the subsoil horizons (B, C and D) (Table 1). We evaluated and derived the capacity of BC and Non-BC contributing to CEC, as expressed by CEC per unit BC or Non-BC. We got CEC per unit BC values of $15\text{-}17.8 \text{ mmol}_C \text{ g}^{-1} \text{ C}$ from depth A to D, and $2.1 \text{ mmol}_C \text{ g}^{-1} \text{ C}$ for Non-BC. Thus the capacity of BC contributing to total soil CEC was 6-9 times higher than Non-BC. The BC in deeper horizons had a 4-19% higher capacity to do so than that in the topsoil horizon A.

3.2 Specific Surface Area and Charge Density

Anthrosol subsoils (B, C, D) have 18-23% higher specific surface area (SSA) than the topsoil horizon A ($25.3 \text{ m}^2 \text{ g}^{-1}$), and at the same time have 20-21% higher clay contents than the topsoil (25.3%) (Table 1). The SSA per unit clay showed less than 2% difference indicating clay is a negligible variable for controlling change of charge density along the depth profile. Charge density, calculated from CEC divided by the SSA, was 31-35% higher in topsoil horizon A than in the subsoil (Table 1). With similar clay content, the 66% higher SSA in Anthrosol top soil than the adjacent soil suggested BC could make a significant contribution to the surface area. Meanwhile, the 156% higher charge density of Anthrosol top soil suggested BC is highly effective in creating CEC compared to clay. The charge density increased slightly by 4% from depth B to D, similar to that of EC to C.

Table 1. Properties of BC-rich anthrosol and adjacent soil at LG site from the central Amazon

ID	Soil Depth m	Sand -----%-----	Silt	Clay	SSA m ² g ⁻¹	CEC mmol _C kg ⁻¹	EC μmol _C m ⁻²	Charge Density μmol _C m ⁻²	C Content mg g ⁻¹	BC fraction % of organic C	BC mg g ⁻¹	Non-BC	CEC _C ^a -----mmol _C g ⁻¹ C-----	CEC _{BC} ^b	CEC _{Non-BC} ^c
Adj.	0-0.08	69.8	4.6	25.6	15.2	69	6	4.5	20.7	9.3	1.9	18.8	3.3	15.0	2.1
A	0-0.16	46.7	28.0	25.3	25.3	292	127	11.5	29.0	62.2	18.0	11.0	10.1	15.0	2.1
B	0.16-0.43	43.4	26.0	30.5	31.0	264	81	8.5	21.3	77.0	16.4	4.9	12.4	15.5	2.1
C	0.43-0.67	44.3	25.3	30.4	30.0	258	86	8.6	19.1	76.2	14.6	4.5	13.5	17.1	2.1
D	0.67-1.20	43.4	26.3	30.4	29.8	262	97	8.8	18.4	77.8	14.3	4.1	14.2	17.8	2.1

Adj.: Adjacent soil; SSA: Specific surface area; EC: Exchangeable cations, Ca, Mg, K, Na
CEC_C^a: CEC per unit soil organic C; CEC_{BC}^b: CEC per unit BC; CEC_{Non-BC}^c: CEC per unit Non-BC

3.3 Carbon Forms on BC Surfaces Determined by NEXAFS

Cluster analyses of C functional groups within soil aggregate sections showed a three-layered pattern of spectrally distinct regions for each BC particle (shown in red, green and yellow), embedded within minerals (Blue) (Fig. 1). The BC inner region (Core, IN=red) with strongly aromatic C features at 285 eV was surrounded by a layer (Intermediate, M=green) with only slightly lower aromatic C and greater peak intensities at 288-289 eV indicating oxidized C functional groups. The spectra of the outer region of BC particles (Outerlayer, OUT=yellow) had distinct features with much lower aromatic C and greater proportions of oxidized C forms (Fig. 1).

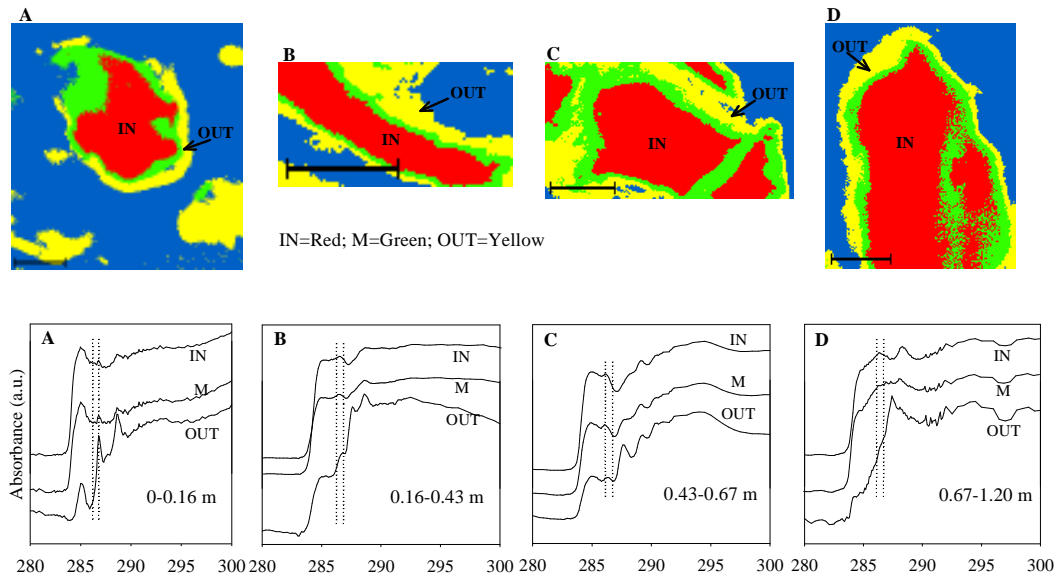


Fig. 1. NEXAFS cluster maps and corresponding spectra of C functional groups for soil aggregate sections from a depth profile of a BC-rich Anthrosol from the Central Amazon (A=topsoil horizon; B, C and D=subsoil horizon with increasing depth).

IN=Red for BC core region; M=Green for intermediate region; OUT=Yellow for BC outerlayer; Blue=organo-mineral mixture. Each scale bar = 2 μm . In spectra, the first line stands for peak at 286.1 eV and the second line stands for peak shifted to higher energy at 286.7 eV, which is characteristic of adsorbed organic materials.

Deconvolution of the NEXAFS spectra of the BC core region yielded 34.7% aromatic C and 39.1% oxidized C (Table 2) in Anthrosol topsoil horizon A. The spectra of the BC outer region had only 4.6% aromatic C but 58.8% of oxidized C, indicating the C on BC surface was highly oxidized. Carbon with similar spectral feature can also be found within the aggregate and minerals (Fig. 1A), suggesting organic matter with high oxidized C spreads within aggregate and minerals. The aromatic C portion (Table 2) was over 2 times higher in the outer region of the BC particles in the subsoil horizons B (16.9%), C (14.2%) and D (15.8%) than in the topsoil horizon A (4.6%), suggesting the C on BC surfaces was more recalcitrant in subsoils than Anthrosol top soil.

Non-BC organic matter including microbial biomass and humic substances extracts showed contrastingly different spectra compared to BC. For bacteria and fungi, only 5.2% and 3.0%

of the total C was resolved as aromatic C (Table 2), respectively. And humic substances extracts have only 10-13% aromatic C (Liang et al., 2008). For top soil A, the carbon signal on BC outerlayer (12.7) is more similar to microbial biomass bacteria (10.8) and fungi (15.7) as reflected by the ratio of oxidized C to aromatic C, suggesting this part of C is most likely adsorption of Non-BC organic matter from the external input. NMR data confirmed highest Non-BC content in the top soil.

Table 2. Carbon functional groups determined by NEXAFS spectral deconvolution within BC-bearing aggregate sections. Reference spectra for microbial biomass were generated in two other studies [16, 18]

Depth (m)	Spatial Location	Aromatic C %	Oxidized C %	Oxidized/Aromatic ratio
A (0-0.16)	Core	34.7	39.1	1.1
	Intermediate	39.6	39.9	1.0
	Outerlayer	4.6	58.8	12.7
B (0.16-0.43)	Core	25.0	40.6	1.6
	Intermediate	22.7	41.1	1.8
	Outerlayer	16.9	49.2	2.9
C (0.43-0.67)	Core	31.7	37.7	1.2
	Intermediate	28.0	39.4	1.4
	Outerlayer	14.2	42.6	3.0
D (0.67-1.2)	Core	27.2	36.2	1.3
	Intermediate	25.5	38.4	1.5
	Outerlayer	15.8	49.1	3.1
Bacteria	Bulk	5.2	56.3	10.8
Fungi	Bulk	3.0	47.5	15.7

The C signal of BC and Non-BC are clearly different [28]. BC showed a distinct peak at 286.1 eV, on the contrary, Non-BC normally showed obvious peak shifts up to 286.7 eV. The Oxidized C to Aromatic C ratio for BC was consistent below 2 for core and intermediate regions and at around 3 for the surface of BC, except for the sample at A horizon. Oxidation is likely to lower the aromatic signal of BC. However, the most oxidized BC does not resemble Non-BC reference samples of humic substances extracts or microbial biomass with a ratio of Oxidized C to aromatic C far above any BC samples up to 10-15. Thus we clearly distinguished the signal of BC and Non-BC, and confirmed that C on BC surfaces in the top horizon came from Non-BC. The subsoil BC spectral characteristics move more to that of oxidized BC, and the oxidation level in the outerlayer increased 3-6% from horizon B (2.9) to D (3.1). Coincidentally, the charge density increased slightly 4% from depth B to D, with a similar trend for EC to C.

3.4 Cation and Carbon Distribution

Superimposing elemental maps of Ca and C obtained by microprobe revealed a clear and close association between their spatial distributions within the studied soil aggregates (Fig. 2). Using line-scans across BC particles within the aggregate section, total C and Ca contents were found to be greater in core regions of BC particles and decreased towards BC surfaces and surrounding mineral, whereas K showed negligible change (Fig. 3).

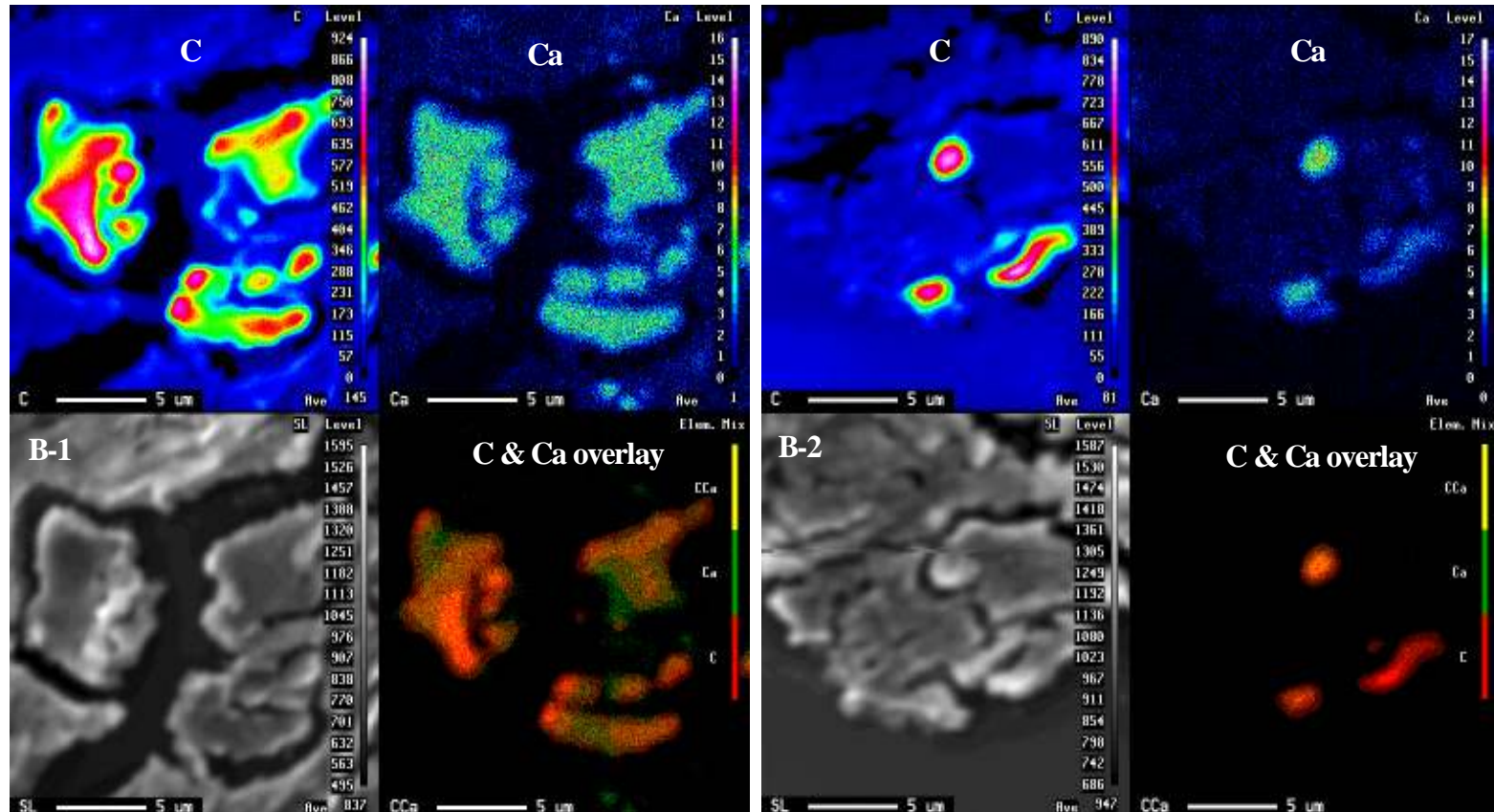


Fig. 2. Microprobe elemental maps for Ca and C and their overlay maps of two soil aggregate sections from subsoil horizon B. The lower left images (B-1 and B-2) are the SEM images of the aggregate sections in grey scale

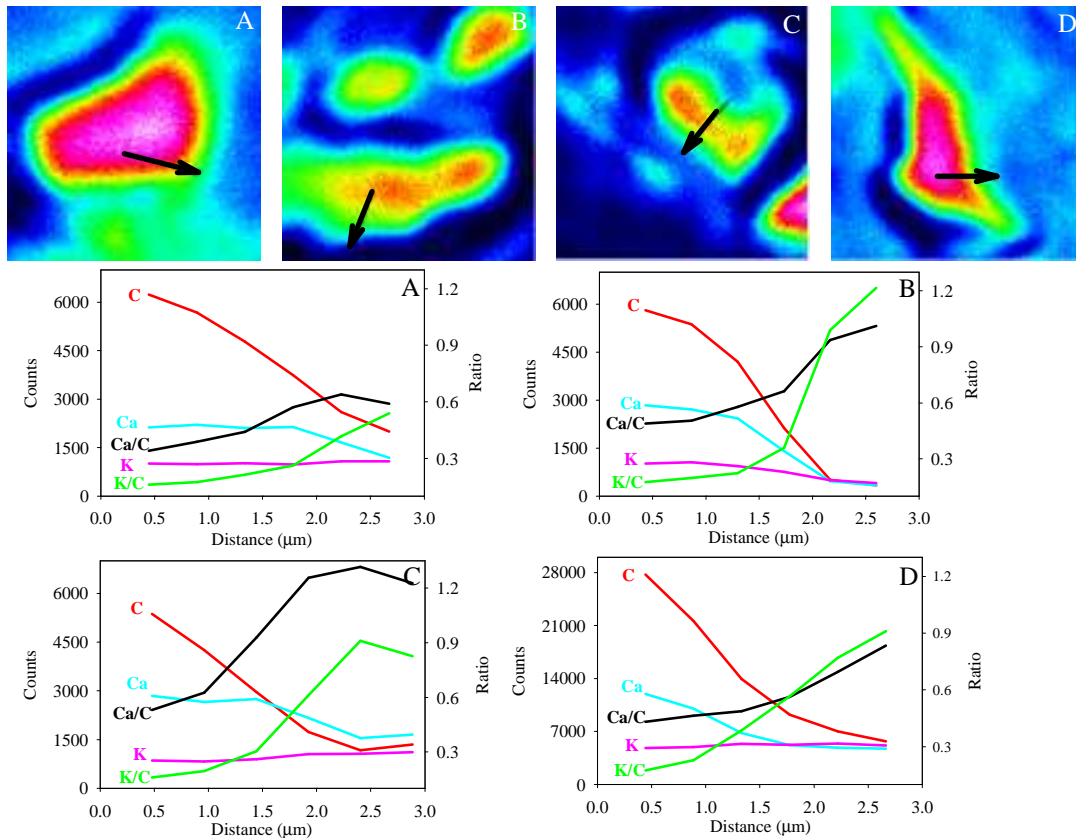


Fig. 3. Microprobe elemental line-scan for C, Ca and K, and cation to C ratios (Ca/C and K/C) across BC particles within soil aggregate sections from a depth profile of a BC-rich Anthrosol from the Central Amazon (A=topsoil horizon; B, C and D=subsoil horizon with increasing depth). Arrows show the direction of the line-scan, originating near the center of the BC particles. Note the differences in y-axis scale of counts for the subsoil horizon D

As an element closely associated with organic matter, it is not surprising to see high Ca contents correlate with high C contents across BC particles. The ratios of Ca to C (Ca/C) and K to C (K/C) were found to be 73-131% and 234-594% higher in the surface regions of BC than that in their core regions, respectively, suggesting that per unit C the surface is better able to retain cations. The ratios of cations to C near these BC particle surfaces were observed to be pronouncedly higher in the subsoil horizons than the topsoil horizon, being 41-108% higher for Ca to C (Ca/C) and 53-126% higher for K to C (K/C), in line with the trend of charge density and EC to C.

3.5 BC Surface Functionality from Oxidation vs. Adsorption

The CEC per unit C at all depths was greater in the BC-rich Anthrosol than in the adjacent soil, which confirms our earlier findings of the enhanced nutrient holding capacity of BC-rich soils [16]. The fact that BC had a 6-9 times higher CEC than Non-BC reinforces the significant role of BC contributing to the total soil CEC in our studied soils.

The CEC per unit C and per unit BC increased with depth, being up to 42% and 19%, respectively, higher in the subsoil than in the topsoil (Table 1). Concurrently, the proportion of BC as a fraction of total C increased. Oxidation of BC surfaces was more effective and important for creating CEC than adsorption of organic matter to BC, especially in deep horizons. Oxidation rather than adsorption of organic matter was also found to be responsible for greater increases in CEC by [29].

This greater proportion of Non-BC near the soil surface appeared to cause more organic matter to sorb onto BC surfaces as demonstrated by the NEXAFS analyses (Table 2). Microbial matter such as bacteria and fungi has an Oxidized/Aromatic C ratio of 10.8 and 15.7, respectively. With an Oxidized/Aromatic C ratio of 12.7, the outer region of BC particles in the topsoil horizon showed a C signature of microbial matter (Table 2), confirming its source originating from adsorbed Non-BC materials. In comparison, the outer region of BC particles in the subsoil horizons showed much greater share of aromatic C. Therefore, the nature of BC particles surface properties changed with depth.

Subsoil horizons with greater CEC per unit C and per unit BC and with lower adsorption of organic matter to BC surfaces were also associated with a higher surface abundance of cations (Fig. 3). This observation provides direct proof for greater cation retention by oxidized surfaces of BC than by adsorption of Non-BC.

The deconvolution of NEXAFS spectra revealed modestly higher proportions of oxidized C (Table 2) on BC surfaces in subsoil horizons than in the topsoil horizon. The greater CEC per unit C in subsoils may therefore not only be a result of a greater level of oxidation of BC surfaces in subsoils, but also of less coating of BC surfaces by Non-BC materials. Organic matter adsorption may decrease accessibility of surface functional groups of BC as well as of inner surfaces and micro- and mesopores of BC. It has been found that adsorbed OM may preferentially clog micropores (<2 nm) in minerals and greatly reduce surface area of mineral assemblages depending on the amount sorbed and the type of minerals [30-32]. Similar processes could have played a role on BC, as activated carbon may have more than 42% and up to 52% of their total porosity as micropores (<2 nm) and mesopores (2-50 nm), respectively [33-35]. The BET N₂ method was found to underestimate internal pore spaces if Non-BC is adsorbed to BC surfaces, as the rigidity of the adsorbed OM may restrict the diffusion of N₂ into the internal microporosity associated with glassy solids [32, 36, 37]. Therefore, surface sorption of Non-BC may have not only clogged pores but also reduced CEC per unit C.

4. CONCLUSIONS

In summary, the high amounts of CEC on BC surfaces likely originate to a greater extent from oxidation of BC than from adsorption of Non-BC. In fact, adsorption of Non-BC to oxidized BC surfaces may have even decreased the CEC of the aged BC. The reactive functional groups on BC surfaces enable binding of cations and explain nutrient retention by BC. Future studies should focus on the real surface nature of BC in terms of their functionality. With its well-documented recalcitrance to microbial decomposition [1, 2, 22, 38, 39], BC may remain in the environment for long periods of time. With prolonged oxidation in the environment, aged BC may have an important role for contaminant adsorption and nutrient retention. Black C may therefore have significant impacts on the environmental behavior of contaminants and solutes for long periods of time after its deposition [40]. In-depth understanding of both biotic and abiotic processes affecting the oxidation of BC may warrant further study.

ACKNOWLEDGEMENTS

This project was funded by the Division of Environmental Biology of the National Science Foundation (NSF) under contract DEB-0425995. Any opinions, findings, and conclusions or recommendations expressed in this material are those of the authors and do not necessarily reflect the views of the National Science Foundation. A small grant was provided by the NSF IGERT program in Biogeochemistry and Environmental Biocomplexity at Cornell University to B. Liang. The NEXAFS spectra were obtained at the National Synchrotron Light Source (NSLS), Brookhaven National Laboratory, a DOE supported facility at the beamline X-1A1 developed by the group of Janos Kirz and Chris Jacobsen at SUNY Stony Brook, with support from the New York State Office of Science and Technology Academic Research and NASA's Discovery Data Analysis and Exobiology programs. The elemental mapping measurements were performed at the Cornell Center for Materials Research at Cornell University (CCMR), which is part of the NSF's MRSEC program. A Distinguished Postdoctoral Scholar Award was provided to B. Liang by Academia Sinica. Many thanks to Drs. Murray McBride, Janice E. Thies for insightful advice, to Janine McGowan for NMR measurement, to Fernando Costa and Manuel Arroyo-Kalin for help with sampling, to Dr. Yuanming Zhang for substantial help with the sectioning on the ultra-microtome, and to Dr. Scott Warren for instruction of surface area measurement.

COMPETING INTERESTS

Authors have declared that no competing interests exist.

REFERENCES

1. Goldberg ED. *Black Carbon in the Environment: Properties and Distribution*. New York: John Wiley & Sons; 1985.
2. Schmidt MWI, Noack AG. Black carbon in soils and sediments: Analysis, distribution, implications, and current challenges. *Glob Biogeochem Cycles*. 2000;14:777–793.
3. Kuhlbusch TAJ. Black carbon and the carbon cycles. *Science*. 1998;280,1903–1904.
4. Schmidt MWI. Carbon budget in the black. *Nature*. 2004;42:305–307.
5. Woolf D, Amonette JE, Street-Perrott FA, Lehmann J, Joseph S. Sustainable biochar to mitigate global climate change. *Nat Commun*. 2010;1:56. doi: 10.1038/ncomms1053.
6. Accardi-Dey A, Gschwend PM. Assessing the combined roles of natural organic matter and black carbon as sorbents in sediments. *Environ Sci Technol*. 2002;36:21–29.
7. Braida WJ, Pignatello JJ, Lu YF, Ravikovitch PI, Neimark AV, Xing BS. Sorption hysteresis of benzene in charcoal particles. *Environ Sci Technol*. 2003;37:409–417.
8. Glaser B, Haumaier L, Guggenberger G, Zech W. The 'Terra Preta' phenomenon: A model for sustainable agriculture in the humid tropics. *Naturwissenschaften*. 2001;88:37–41.
9. Lehmann J, da Silva JP, Steiner C, Nehls T, Zech W, Glaser B. Nutrient availability and leaching in an archaeological Anthrosol and a Ferralsol of the Central Amazon basin: Fertilizer, manure and charcoal amendments. *Plant Soil*. 2003;249:343–357.
10. Yang Y, Sheng G. Enhanced pesticide sorption by soils containing particulate matter from crop residue burns. *Environ Sci Technol*. 2003;37:3635–3639.

11. Lohmann R, MacFarlane JK, Gschwend PM. Importance of black carbon to sorption of native PAHs, PCBs, and PCDDs in Boston and New York Harbor Sediments. *Environ Sci Technol*. 2005;39:141–148.
12. Jonker MTO, Hoenderboom AM, Koelmans AA. Effects of sedimentary sootlike materials on bioaccumulation and sorption of polychlorinated biphenyls. *Environ Toxicol Chem*. 2004;23:2563–2570.
13. Wang HL, Lin KD, Hou ZN, Richardson B, Gan J. Sorption of the herbicide terbuthylazine in two New Zealand forest soils amended with biosolids and biochars. *J Soils Sediments*. 2010;10:283–289.
14. Chen BL, Yuan MX. Enhanced sorption of polycyclic aromatic hydrocarbons by soil amended with biochar. *J Soils Sediments*. 2011;11:62–71.
15. Pietikäinen J, Kiikkilä O, Fritze H. Charcoal as a habitat for microbes and its effect on the microbial community of the underlying humus. *Oikos*. 2000;89:231–242.
16. Liang B, Lehmann J, Solomon D, Kinyangi J, Grossman J, O'Neill B, et al. Black carbon increases cation exchange capacity in soils. *Soil Sci Soc Am J*. 2006;70:1719–1730.
17. Cheremisinoff PN, Ellerbusch F. *Carbon Adsorption Handbook*. Ann Arbor, MI: Ann Arbor Science Publishers; 1978.
18. Lehmann J, Liang BQ, Solomon D, Lerotic M, Luizão F, Kinyangi J, et al. Near-edge X-ray absorption fine structure (NEXAFS) spectroscopy for mapping nano-scale distribution of organic carbon forms in soil: Application to black carbon particles. *Glob Biogeochem Cycles*. 2005;19:GB1013.
19. Sombroek WG, Nachtergaele FO, Hebel A. Amounts, dynamics and sequestering of carbon in tropical and subtropical soils. *Ambio*. 1993;22:417–426.
20. Skjemstad JO, Taylor JA, Smernik RJ. Estimation of charcoal (char) in soils. *Comm Soil Sci Plant Nutr*. 1999;30:2283–2298.
21. Nelson PN, Baldock JA. Estimating the molecular composition of a diverse range of natural organic materials from solid-state ¹³C NMR and elemental analyses. *Biogeochemistry*. 2005;72:1–34.
22. Liang B, Lehmann J, Solomon D, Sohi S, Thies JE, Skjemstad JO, et al. Stability of biomass-derived black carbon in soils. *Geochim Cosmochim Acta*. 2008;72:6069–6078.
23. Lehmann J, Kinyangi J, Solomon D. Organic matter stabilization in soil microaggregates: implications from spatial heterogeneity of organic carbon contents and carbon forms. *Biogeochemistry*. 2007;85:45–57.
24. Jacobsen C, Feser M, Lerotic M, Vogt S, Maser J, Schäfer T. Cluster analysis of soft x-ray spectromicroscopy data. *J Phys IV*. 2003;104:623–626.
25. Lerotic M, Jacobsen C, Gillow JB, Francis AJ, Wirick S, Vogt S, et al. Cluster analysis in soft X-ray spectromicroscopy: Finding the patterns in complex specimens. *J Electron Spectrosc Relat Phenom*. 2005;144–147:1137–1143.
26. Ravel B, Newville M. Athena, artemis, hephaestus. *J Synchrotron Rad*. 2005;12:537–541.
27. Schumacher M, Christl I, Scheinost AC, Jacobsen C, Kretzschmar R. Heterogeneity of water-dispersible soil colloids investigated by Scanning Transmission X-ray Microscopy and C-1s XANES microspectroscopy. *Environ Sci Technol*. 2005;39:9094–9100.
28. Solomon D, Lehmann J, Kinyangi J, Liang B, Heymann K, Dathe L, et al. Carbon (1s) NEXAFS Spectroscopy of Biogeochemically Relevant Reference Organic Compounds. *Soil Sci Soc Am J*. 2009;73:1817-1830.

29. Cheng CH, Lehmann J, Engelhard MH. Natural oxidation of black carbon in soils: Changes in molecular form and surface charge along a climosequence. *Geochim Cosmochim Acta*. 2008;72:1598–1610.
30. Kaiser K, Guggenberger G. Mineral surfaces and soil organic matter. *Eur J Soil Sci*. 2003;54:219–236.
31. Mikutta C, Lang F, Kaupenjohann M. Soil organic matter clogs mineral pores: evidence from ¹H-NMR and N₂ adsorption. *Soil Sci Soc Am J*. 2004;68:1853–1862.
32. Kwon S, Pignatello JJ. Effect of natural organic substances on the surface and adsorptive properties of environmental black carbon (char): pseudo pore blockage by model lipid components and its implications for N₂-probed surface properties of natural sorbents. *Environ Sci Technol*. 2005;39:7932–7939.
33. Wu FC, Tseng RL, Hu CC. Comparisons of pore properties and adsorption performance of KOH-activated and steam-activated carbons. *Micropor Mesopor Mat*. 2005;80:95–106.
34. Wu FC, Tseng RL, Hu CC, Wang CC. The capacitive characteristics of activated carbons—comparisons of the activation methods on the pore structure and effects of the pore structure and electrolyte on the capacitive performance. *J Power Sources*. 2006;159:1532–1542.
35. Tseng RL, Tseng SK, Wu FC. Preparation of high surface area carbons from Corn cob with KOH etching plus CO₂ gasification for the adsorption of dyes and phenols from water. *Colloid Surfaces A*. 2006;279:69–78.
36. Xing B, Pignatello JJ. Dual-mode sorption of low-polarity compounds in glassy poly(vinyl chloride) and soil organic matter. *Environ Sci Technol*. 1997;31:792–799.
37. de Jonge H, de Jonge LW, Mittelmeijer-Hazeleger MC. The microporous structure of organic and mineral soil materials. *Soil Sci*. 2000;165:99–108.
38. Cheng CH, Lehmann J, Thies JE, Burton S. Stability of black carbon in soils across a climatic gradient. *J Geophys Res*. 2008;113:G02027.
39. Kuzyakov Y, Subbotina I, Chen H, Bogomolova I, Xu X. Black carbon decomposition and incorporation into soil microbial biomass estimated by ¹⁴C labeling. *Soil Biol Biochem*. 2009;41:210–219.
40. Redell CJ, Elmore AC, Burken JG, Stringer RD. Waterjet injection of powdered activated carbon for sediment remediation. *J Soils Sediments*. 2011;11:1115–1124.

© 2013 Liang et al.; This is an Open Access article distributed under the terms of the Creative Commons Attribution License (<http://creativecommons.org/licenses/by/3.0>), which permits unrestricted use, distribution, and reproduction in any medium, provided the original work is properly cited.

Peer-review history:

The peer review history for this paper can be accessed here:
<http://www.sciencedomain.org/review-history.php?iid=218&id=10&aid=1217>